OFFICE OF NAVAL RESEARCH

CONTRACT NO. N00014-86-K-0772

TECHNICAL REPORT NO. 33

# The Effect of Deformation History on The Morphology and Properties of Blends of Polycarbonate and a Thermotropic Liquid Crystalline Polymers

by

A. Kohli, N. Chung, and R. A. Weiss

Liquid Crystalline Polymer Research Center
University of Connecticut
Storrs, CT 06269-3136

Prepared for Publication

in

Polymer Engineering and Science

January 11, 1989

Unclassified
SECURITY CLASSIFICATION OF THIS PAGE

# REPORT DOCUMENTATION PAGE

| | |
|---|---|
| 1a REPORT SECURITY CLASSIFICATION: Unclassified | 1b RESTRICTIVE MARKINGS: None |
| 2a SECURITY CLASSIFICATION AUTHORITY | 3 DISTRIBUTION/AVAILABILITY OF REPORT: Approved for Public Release, Distribution Unlimited |
| 2b DECLASSIFICATION/DOWNGRADING SCHEDULE | |
| 4 PERFORMING ORGANIZATION REPORT NUMBER(S): Technical Report No. 33 | 5 MONITORING ORGANIZATION REPORT NUMBER(S) |
| 6a NAME OF PERFORMING ORGANIZATION: University of Connecticut; 6b OFFICE SYMBOL (If applicable) | 7a NAME OF MONITORING ORGANIZATION: Office of Naval Research |
| 6c ADDRESS (City, State, and ZIP Code): Storrs, CT 06268 | 7b ADDRESS (City, State, and ZIP Code): 800 North Quincy Avenue Arlington, VA 22217 |
| 8a NAME OF FUNDING/SPONSORING ORGANIZATION; 8b OFFICE SYMBOL (If applicable): ONR | 9 PROCUREMENT INSTRUMENT IDENTIFICATION NUMBER: N00014-86-K-0772 |
| 8c ADDRESS (City, State, and ZIP Code): 800 North Quincy Avenue Arlington, VA 22217 | 10 SOURCE OF FUNDING NUMBERS: PROGRAM ELEMENT NO. / PROJECT NO. / TASK NO. / WORK UNIT ACCESSION NO |

11 TITLE (Include Security Classification)
The Effect of Deformation History on the Morphology and Properties of Blends of Polycarbonate and a Thermotropic Liquid Crystalline Polymers (Unclassified)

12 PERSONAL AUTHOR(S)
A. Kohli, N. Chung, and R. A. Weiss

| 13a TYPE OF REPORT | 13b TIME COVERED | 14 DATE OF REPORT (Year, Month, Day) | 15 PAGE COUNT |
|---|---|---|---|
| Interim Technical | FROM ____ TO 1-11-89 | 1989-1-11 | 40 |

16 SUPPLEMENTARY NOTATION
Submitted to Polymer Engineering and Science (LCPRC Publication No. 89-02)

| 17 COSATI CODES | | | 18 SUBJECT TERMS (Continue on reverse if necessary and identify by block number) |
|---|---|---|---|
| FIELD | GROUP | SUB GROUP | Liquid Crystalline Polymers, and Polymer Blends. |
| | | | |
| | | | |

19 ABSTRACT (Continue on reverse if necessary and identify by block number)

The addition of an immiscible LCP phase improves the melt processability of a host thermoplastic polymer. In addition, by employing a suitable deformation history, the LCP phase may be elongated and oriented such that a microfibrillar morphology can be retained in the solid state. This has important ramifications for the development of self-reinforcing polymer blends to compete with conventional inorganic fiber-reinforced polymers. Shear flows are generally ineffective at developing these morphologies, but flows that incorporate an extensional region, such as the converging flow found at the entrance to a capillary or die can produce an elongated LCP phase. Simple extensional flows, such as melt drawing, are most effective at producing LCP microfibrils, and their efficiency increases with increasing draw ratio. The moduli of highly drawn blends were well approximated by a composite's analogy of long uniaxially oriented LCP fibers in a PC matrix.

| 20 DISTRIBUTION/AVAILABILITY OF ABSTRACT | 21 ABSTRACT SECURITY CLASSIFICATION | |
|---|---|---|
| ☒ UNCLASSIFIED/UNLIMITED ☐ SAME AS RPT ☐ DTIC USERS | Unclassified | |
| 22a NAME OF RESPONSIBLE INDIVIDUAL: Dr. Kenneth J. Wynne | 22b TELEPHONE (Include Area Code): (202) 696-4410 | 22c OFFICE SYMBOL: ONR |

DD FORM 1473, 84 MAR — 83 APR edition may be used until exhausted. All other editions are obsolete.

SECURITY CLASSIFICATION OF THIS PAGE
Unclassified

Final

# THE EFFECT OF DEFORMATION HISTORY ON THE MORPHOLOGY AND PROPERTIES OF BLENDS OF POLYCARBONATE AND A THERMOTROPIC LIQUID CRYSTALLINE POLYMERS

BY

A. KOHLI*, N. CHUNG, AND R. A. WEISS**

DEPARTMENT OF CHEMICAL ENGINEERING AND
LIQUID CRYSTALLINE POLYMER RESEARCH CENTER
UNIVERSITY OF CONNECTICUT
STORRS, CT 06269-3136

* Current Address: IBM Corporation
1701 North Street
Endicott, NY 13760

** To whom correspondence should be sent.

## INTRODUCTION

Interest in thermotropic liquid crystalline polymers (LCP) has grown in recent years due to their inherently high stiffness and strength, high use temperatures, excellent chemical resistance, low melt viscosity and low coefficient of expansion. However, despite extensive research and development, as well as several recent commercializations, LCP's currently have relatively few established commercial markets. The materials tend to be expensive due primarily to high monomer costs. As a result, the developing applications are relatively low volume ones where the LCP's enjoy clear-cut advantages over the more conventional materials. For example, LCP's have realized their greatest success not in applications requiring high modulus and strong materials, but rather in the production of intricate moldings where the ability to fill the mold and dimensional stability of the part are the crucial specifications.

Blending LCP's with other, less expensive thermoplastics offers the possibility for exploiting many of their desirable characteristics, but at a reduced material cost. It is not surprising, therefore, that a growing interest in LCP/polymer blends has developed in recent years (1). The work of a number of laboratories has been directed at developing compositions in which a discrete LCP phase functions both as a processing aid and as a solid-state reinforcement (2-10). At elevated temperature, the melt viscosity is lowered by the presence of an LCP dispersed phase. During processing of the blend, it is possible to deform and orient the LCP phase such that the solidified compound contains a microfibrillar LCP phase. The morphology and properties of such blends are similar in many respects to more conventional short-fiber reinforced plastics. As such, LCP/polymer blends may be effective for improving the dimensional stability of thermoplastic films or moldings, or they may be competitive with glass fiber-reinforced plastics in applications where processability and low density are key requirements.

Previous work in our laboratory (5) has demonstrated the feasibility of using the addition of an LCP to a thermoplastic in order to both improve processability and to form in situ a reinforcing phase. In that study, it was concluded that orientation and deformation of the LCP dispersed phase was necessary for both effects. The reinforcing phase consisted of LCP microfibrils with diameters and aspect ratios of the order of μm's and 100, respectively. The objective of the research described herein was to assess the effect of deformation history on the morphology and properties of LCP/polymer blends. Specifically, the relative importance of extensional and simple shear flows on the development of a microfibrillar LCP domain structure was investigated.

## EXPERIMENTAL

The thermotropic liquid crystalline polymer, Vectra RD500,

was kindly provided by Dr. Larry F. Charbonneau of Hoechst-Celanese Corporation. It was a terpolymer comprised of 52 mole% 4-hydroxybenzoic acid (HBA), 28 mole% 6-hydroxy-2-naphthoic acid (HNA), 10 mole% terephthalic acid, and 10 mole% hydroquinone. The inherent viscosity at 25°C for 0.1 wt% concentration in a 1:1 mixture of pentafluorophenol: hexafluoropropanol was 3.08 (11). The polycarbonate (PC) used had a number average molecular weight of 16,000 and weight average molecular weight of 34,000 as determined by gel permeation chromatography.

Blends of LCP and PC ranging in composition from 5 - 80 wt% LCP were prepared by melt blending at 270°C with a Custom Scientific Instruments (CSI) Max-mixing extruder. Before blending, the neat polymers were dried in a vacuum oven at 115°C for at least 24 hours. The CSI extruder was also used with a take up device to prepare melt drawn fibers.

Transition temperatures of the blends as well as the neat polymers were measured with a Perkin-Elmer DSC 7 differential scanning calorimeter equipped with a mechanical cooling accessory, a TAC 7 thermal analysis instrument controller, and a PE 7500 professional computer. In order to remove any previous thermal histories, all the samples were initially scanned from 30°C to 290°C at a heating rate of 20°C/minute and then quenched as rapidly as possible in the instrument. All subsequent heating and cooling scans were made at a rate of 20°C/min. Samples of 9-13 mg were encapsulated in aluminum pans and the measurements were made under a nitrogen atmosphere.

Shear viscosity measurements were made with a Rheometrics System 4 mechanical spectrometer using a cone and plate geometry. The cone had an angle of 0.1 radians and a diameter of 25 mm. The shear rate range covered was from 0.01 to 10.0 $s^{-1}$. The experiments were conducted in a gas convection environmental chamber at 270°C. For higher shear rates, viscosity measurements were made with an Instron capillary viscometer. All experiments were done at 270°C and at least three experiments on fresh samples were made for each composition. A capillary with L/D = 40 and D = 1.27 mm was used. Entrance pressure corrections were neglected, but the Rabinowitsch correction for non-Newtonian behavior was applied. For the morphology studies, capillaries with L/D = 20 and 10 were also used.

Scanning electron micrographs of fracture surfaces of the blends were obtained with an AMR model 1200 scanning electron microscope (SEM). The samples were fractured under tension in liquid nitrogen and sputter coated with a 10 nm thick layer of gold in order to provide a conductive path. In order to preserve the structure of the melt formed during the rheological measurements, the samples were quenched in ice water. In the case of the capillary experiments, this simply required extrusion into ice water. For the cone and plate experiments, it required quickly removing the fixtures after stopping the flow and placing the cone and plate sandwich into ice water. This generally took less than one minute after the cessation of shearing.

Dynamic mechanical measurements were made with a Polymer Laboratories Dynamic Mechanical Thermal Analyzer (DMTA) using the tensile mode. Bar specimens, about 5 mm x 1 mm x 2 mm, were cut form compression molded films and fiber specimens, about 0.1 mm diameter, were used for the drawn samples. All measurements were made with a frequency of 1 Hz and a strain amplitude of 0.3%.

## RESULTS AND DISCUSSION

The DSC thermograms of the blends as well as the neat polymers are shown in Fig. 1. The glass transition temperatures of the LCP and the PC were 101°C and 147°C, respectively, and the crystalline to nematic transition (K -> N) for the LCP was about 236°C. The nematic nature of the LCP mesophase was confirmed by a threaded-Schileren texture observed by polarized optical microscopy. The nematic to isotropic transition was not observed before decomposition of the LCP occurred.

The composition dependence of the transitions is shown in Fig. 2 for two different thermal histories: (1) after quenching rapidly from 290°C and (2) after cooling at 20°C/min from 270°C. The thermal data are summarized in Tables 1-3. The cooling data showed a considerable super-cooling of the N -> K transition and the two Tg's. The K -> N transition of the LCP remained constant in the blends at the same temperature as for the pure LCP. Although the enthalpy change was dependent on the sample's thermal history, the position of the endotherm was not. The enthalpy of the N -> K transition increased when the slower cooling rate was used and the effect was greater at the lower LCP concentrations. The Tg(PC) was relatively unaffected by thermal history of the blend. Tg(LCP), however, increased when the cooling rate was lowered. Both Tg's were slightly composition dependent, though it was not clear whether this was due to some miscibility or to phase size. Empirical fits of the Fox equation (12) to the Tg-composition data yielded an estimate of about 2% miscibility of the LCP in PC. The effect of annealing the blends at 145°C on the transitions is shown in Fig. 3. The K -> N transition at 236°C became narrower and at least two other endothermic events were observed, a lower temperature peak near 200°C and a shoulder on the low temperature side of the upper endothermic peak. The latter was most noticeable in the pure LCP. Although the morphologies associated with the various transitions were not identified, these observations were consistent with that of a fast and a slow crystallization process reported for HBA/HNA copolymers (13).

The viscosity versus shear rate data at 270°C for the starting materials and the blends are given in Fig. 4. In all cases, over the entire shear rate range studied, the melt viscosity was lowered by the addition of the LCP. The overlap of the viscosity data obtained from the cone and plate rheometer and the capillary viscometer was poor. In general, the viscosities determined from the capillary at low shear rates were higher than those measured with the cone and plate for high shear rates.

This was not too surprising since as will be shown below the shape and size of the dispersed phase was dependent not only on the rate of deformation, but also on the instrument used to measure the viscosity. Although both instruments yield a simple shear flow field, the simple shear flow in the capillary is preceded by a region of partial extensional flow at the capillary entrance. This had a significant effect on the dispersed phase morphology.

The capillary viscometer data in Fig. 4 were consistent with other capillary studies (3-10) that also showed that relatively low concentrations of LCP dramatically lowered the melt viscosities of thermoplastics. This effect is clearly shown in Fig. 5 in which the melt viscosity at a shear rate of 150 $s^{-1}$ is plotted against the blend composition. The melt viscosities of the blend decreased monotonically with increasing LCP content. For example, the addition of 5% and 10% LCP to PC lowered the melt viscosity by 54% and 75%, respectively. Over the entire range of composition the viscosity changed by nearly two orders of magnitude.

The data for the cone and plate geometry also showed a lowering of the viscosity by the addition of the LCP. This agreed with the results of Blizard and Baird (6), but were inconsistent with those of Weiss et al. (5). In the latter study, the authors found that for steady shear flows without pre-extension, the addition of an LCP phase in a polystyrene melt increased the melt viscosity. Microscopic evaluation of those blends revealed that the dispersed LCP phase was not deformed by the shear flow. They concluded that it was necessary to deform the dispersed phase in order to attain a lowering of the viscosity, and they also concluded that an extensional component of stress was necessary for deforming the LCP phase. Those findings were consistent with fluid dynamic theories that predict a viscosity increase for flows in which the dispersed phase is not deformed (13). The reason for the different results reported here is not understood and is the subject of current studies in our laboratory.

The viscosity curves for the blends containing up to 20% LCP reflected the viscosity-shear rate characteristics of the PC. At low shear rates, the curves were Newtonian, though shear thinning was observed at the higher shear rates. The magnitude of the shear thinning increased and the shear rate for the onset of shear thinning decreased with increasing LCP concentration. The flow curves for the higher LCP compositions were more typical of that of the pure LCP in that no clear Newtonian region was observed. Based on the SEM micrographs of the blend morphologies, Fig. 6, it appeared that phase inversion occurred between 40 - 60% (wt) LCP. Below 40% LCP, the morphology consisted of spherical LCP domains, 1 - 10 μm in diameter, dispersed in the PC continuous phase. Two different regions were observed in the 40% LCP blend. One region was PC-rich and contained spherical LCP domains; the other region had a fibrous

texture characteristic of the pure LCP. Above 60% LCP, the blend morphology was fibrous and similar to that of the pure LCP. In those samples, it was not possible to distinguish the two phases.

The morphology of a 20% LCP/80% PC blend resulting from simple shear melt flow is shown in Fig. 7 as a function of rate of deformation. In agreement with theories for two-phase suspensions, simple shear flow was not effective at deforming or orienting the LCP domains. The morphology following simple shear was characterized by μm-sized spherical domains of the LCP. Increasing the shear rate reduced the domain size, but did not greatly deform the phase.

Fig. 8 shows the effect of deformation rate and the capillary aspect ratio (L/D) on the morphology of the 20% LCP/80% PC blend. Fluid dynamic theories predict that the LCP dispersed phase elongates into a fibrillar phase at the entrance of the capillary. This is the consequence of the extensional stresses due to the converging flow at the entrance. In the shear region of the capillary, however, the elongated phase either relaxes back to a spherical shape or breaks up into smaller spherical droplets as a consequence of a competition between viscous and interfacial forces. The microphotographs in Fig. 8 are consistent with these predictions. For high L/D and low deformation rate, the LCP domains were spherical with no visible orientation. As the capillary aspect ratio decreased and the deformation rate increased, the LCP domains became more elongated with a preferential orientation parallel to the machine direction. The effect of increasing deformation rate was to more effectively elongate the LCP phase in the entrance region. In the capillary, the elongated LCP phase either relaxed or broke-up into spherical or ellipsoidal droplets, and the efficiency of this increased with increasing capillary length. Therefore in order to develop and maintain dispersed LCP microfibrils in these blends, high extrusion rates and very short dies were required.

The effect of simple extension of the melt on the blend morphology is also shown in Fig. 8 for comparison. This morphology was obtained by manually pulling and then freezing the extrudate from the capillary viscometer. In this case, well developed LCP microfibrils with relatively high aspect ratios were formed. The orientation in the drawing direction was very high.

The influence of the draw ratio (DR) on the effectiveness of microfibril formation is shown for a 10% LCP/90% PC blend in Fig. 9. DR was calculated from the ratio of the diameter of the drawn blend fiber to that of the extruder die. At a relatively low draw ratio, DR = 50, the LCP phase was only slightly elongated. The microfibers formed were not well developed and had fairly low aspect ratios. An order of magnitude increase in DR (DR = 500) yielded well developed microfibrils oriented parallel to the draw direction.

Drawing also had a significant effect on the fibrous morphology of the 40%PC/60%LCP blend, where the LCP was the continuous phase, Fig. 9(b). For that material, the compression molded specimen already had a fibrous texture, cf. Fig. 6. Melt drawing the blend perfected and oriented the supermolecular fibrils with the effect becoming more significant as the draw ratio increased.

The DMTA data for the compression molded PC, LCP and their blends are given in Fig. 10. The modulus of the LCP below 120°C was about twice that of the PC. Although the addition of the LCP to the PC increased the modulus, the increase was relatively small (e.g., only about 10% for the 60%PC/40%LCP sample). This was a consequence of the spherical morphology of the dispersed phase, which is not efficient as a fiber in contributing to the load bearing capacity of a blend.

The DMTA behavior of the PC showed a large drop in modulus and a peak in tan $\delta$ at about 170°C which corresponded to the glass transition of the PC. The higher value for the transition versus that measured by DSC, cf. Fig. 2, was due to the higher experimental rate. The LCP exhibited two transitions, a minor one at about 120°C corresponding to the glass transition and a major one between 200-250°C corresponding to the K -> N transition. The latter transition was not sharp and probably reflected both the kinetic aspect of this transition and a distribution of phase sizes.

The DMTA thermograms of the blends containing less than 40% LCP exhibited only the response of the PC. Neither the Tg, nor the K -> N transition of the LCP were detected. This again was probably a consequence of a morphology characterizaed by spherical LCP domains in a PC matrix. The domains carried little load and their effect on the mechanical response was minimal.

Between an LCP concentration of 40% and 60% phase inversion occurred, cf. Fig. 6, and the effects of both the PC and LCP phases were observed in the DMTA thermograms. A small drop in the moduli of the blends and a small tan $\delta$ peak (see insert in Fig. 10(b)) were observed at the Tg of the LCP. Another decrease in the moduli and a larger tan $\delta$ peak occurred at the Tg of the PC phase, and a plateau-like region in E' was observed above the PC Tg as a consequence of the crystallinity of the LCP phase.

Melt drawing the polymers and the blends resulted in substantial increase in the tensile modulus. This is shown for the 90%PC/10%LCP blend in Fig. 11. In this case, E' increased by about a factor of six compared with that of a compression molded sample. This increase in stiffness can be attributed to increases of the stiffness of both the PC and LCP phases as shown in Table 4, though the increase of the LCP modulus is much more significant.

Whereas, the addition of the LCP did not greatly enhance the modulus of PC for the compression molded specimens, the modulus increases for the drawn samples were significant. This was due to the change in the morphology from a spherical dispersed phase to microfibrils, cf. Fig. 9. This is demonstrated by comparing the moduli values in Table 4 to predictions for particulate and fiber-reinforced plastics, Fig. 12. Typical lower and upper-bound equations for the modulus of composite materials are given in equation (1) and (2),

$$\text{Lower Bound:} \quad E_c = \frac{E_1 E_2}{E_1 V_2 + E_2 V_1} \tag{1}$$

$$\text{Upper Bound:} \quad E_c = V_1 E_1 + V_2 E_2 \tag{2}$$

where $E_c$ = composite modulus and $V_i$ and $E_i$ are the volume frations and moduli of the two components, 1 and 2 (14). Equation (1) corresponds to a model in which the stresses in the two phases are the same, i.e., isostress model, and equation (2) is an isostrain model. The former is expected for particulate composites and the latter is the case for continuous fiber-reinforcement. Although, the LCP microfibrils in the drawn blends are not continuous, for sufficiently high fiber aspect ratios equation (2) was a reasonable approximation for the modulus of a discontinuous (short) fiber-reinforced plastic.

Volume fractions were calculated from the mass fractions using specific gravities for the PC and LCP of 1.2 (15) and 1.4 (16), respectively. Comparisions between the predictions of equations (1) and (2) and the experimental data are shown in Fig. 12. The agreement was reasonably good for both the drawn and compression molded samples. In both cases, the largest deviation was for the 40%PC/60%LCP blend which fell below the curves for both types of specimens. Phase inversion occurred in this sample and the disagreement between the prediction and the data probably represents an oversimplification of the mechanics of this system by the upper and lower bound predictions. In any event, it appears that the properties and morphology of these blends may be well represented by the composites analogy described above. In addition, it is worth noting that the complicated modulus versus composition behavior, i.e., with local maxima and minima, reported by Isayev and Modic (7) for PC/LCP blends was not observed in this study.

## CONCLUSION

The addition of an immiscible LCP phase improves the melt processability of a host thermoplastic polymer. In addition, by employing a suitable deformation history, the LCP phase may be elongated and oriented such that a microfibrillar morphology can be retained in the solid state. This has important ramifications

for the development of self-reinforcing polymer blends to compete with conventional inorganic fiber-reinforced polymers. Shear flows are generally ineffective at developing these morphologies, but flows that incorporate an extensional region, such as the converging flow found at the entrance to a capillary or die can produce an elongated LCP phase. Simple extensional flows, such as melt drawing, are most effective at producing LCP microfibrils, and their efficiency increases with increasing draw ratio. The moduli of highly drawn blends were well approximated by a composite's anology of long uniaxially oriented LCP fibers in a PC matrix.

ACKNOWLEDGEMENT

This work was supported by DARPA (Grant #ONR N00014-86-K-0772), by the Connecticut Dept. of Higher Education, and by Eastman Kodak Corporation. We are especially indebted to Dr. Larry Charbonneau and the Hoechst-Celanese Corporation for the donation of the liquid crystalline polymer.

## REFERENCES


1. R. A. Weiss and A. Kohli, review article in preparation.

2. F. N. Coggwell, B. P. Griffin, and J. B. Rose, U. S. Patents 4, 386, 174 (1983); 4, 433, 083 (1984); 4, 438, 236 (1984).

3. A. Siegmann, A. Dagan, and S. Koenig, Polymer, 26, 1325 (1985).

4. G. Kiss, Polym. Eng. Sci., 27, 410 (1987).

5. R. A. Weiss, W. Huh, and L. Nicolais, Polym. Eng. Sci., 27, 684 (1987).

6. K. G. Blizard and D. G. Baird, Polym. Eng. Sci., 27, 653 (1987).

7. A. I. Isayev and M. J. Modic, Polym. Composites, 8, 158 (1987).

8. D. Acierno, E. Amendola, C. Carfagna, L. Nicolais, and R. Nobile, Mol. Cryst. Liq. Cryst., 153, 533 (1987)

9. T. Chung, Plastics Eng., Oct. 1987, p.39.

10. R. A. Weiss, W. Huh, and L. Nicolais, in "High Modulus Polymers," A. E. Zachariades and R. S. Porter, Eds., Marcel Dekker, Inc., NY, 1988, p.145.

11. L. F. Charbonneau, personal communication (1987).

12. T. G. Fox, Bull. Amer. Phys. Soc., 1, 123 (1956)

13. H. L. Goldsmith and S. G. Mason in Rheology, v.4, F. R. Eirich, Ed., Academic Press, 1967, p.85.

14. L. E. Nielsen, "Mechanical Properties of Polymers and Composites," v.2, Marcel Dekker, NY, 1974.

15. Modern Plastics Encyclopedia, McGraw Hill Publ., NY, 1984.

16. Hoechst-Celanese product information for Vectra® LCP's.

Table 1. Thermal data for DSC heating thermograms of quenched LCP/PC blends.

| Wt% LCP | $T_g$PC(°C) | $T_g$LCP(°C) | $T_m$,onset(°C) | $T_m$, peak(°C) | ΔH(J/G) |
|---|---|---|---|---|---|
| 0 | 147 | - | - | - | - |
| 5 | 147 | - | 227 | 235 | 0.041 |
| 10 | 146 | - | 226 | 235 | 0.130 |
| 20 | 146 | - | 225 | 236 | 0.330 |
| 40 | 145 | 98 | 225 | 236 | 0.985 |
| 60 | 143 | 99 | 223 | 236 | 1.670 |
| 80 | 140 | 101 | 222 | 235 | 2.370 |
| 100 | - | 101 | 223 | 236 | 3.340 |

Table 2. Thermal data for DSC cooling thermograms (20°C/min) of LCP/PC blends.

| Wt% LCP | $T_g$PC(°C) | $T_g$LCP(°C) | $T_c$onset(°C) | $T_c$ peak(°C) | ΔH(J/G) |
|---|---|---|---|---|---|
| 0 | 145 | - | - | - | - |
| 5 | 142 | - | 202 | 193 | -0.089 |
| 10 | 143 | - | 200 | 194 | -0.232 |
| 20 | 141 | - | 200 | 193 | -0.589 |
| 40 | 141 | 95 | 205 | 196 | -1.299 |
| 60 | 137 | 94 | 206 | 195 | -1.753 |
| 80 | 131 | 94 | 219 | 197 | -2.517 |
| 100 | - | 95 | 198 | 195 | -3.364 |

Table 3. Thermal data for DSC heating thermograms of LCP/PC blends after cooling at 20°C/min.

| Wt% LCP | $T_g$PC(°C) | $T_g$LCP(°C) | $T_m$onset(°C) | $T_m$ peak(°C) | ΔH(J/G) |
|---|---|---|---|---|---|
| 0 | 150 | - | - | - | - |
| 5 | 148 | 109 | 229 | 237 | 0.128 |
| 10 | 147 | 109 | 229 | 238 | 0.325 |
| 20 | 146 | 107 | 226 | 237 | 0.605 |
| 40 | 146 | 107 | 229 | 238 | 1.400 |
| 60 | 143 | 105 | 227 | 237 | 2.132 |
| 80 | 137 | 104 | 229 | 238 | 2.590 |
| 100 | - | 105 | 227 | 238 | 3.460 |

Table 4. Dynamic tensile moduli at 43°C (f = 1 Hz) for Compressin Molded and Melt Drawn LC/LCP blends.

| Wt% LCP | E'(GPa) Compression Molded | Melt Drawn* |
|---|---|---|
| 0 | 0.72 | 2.2 |
| 10 | 0.74 | 4.4 |
| 20 | 0.68 | 7.1 |
| 40 | 0.79 | 11.5 |
| 60 | 0.81 | 14.1 |
| 100 | 1.48 | 26.4 |

* DR = 1000 - 1600

## FIGURE CAPTIONS

Fig. 1. DSC heating thermograms of PC, LCP and their blends after quenching samples from 290°C. The numbers in parentheses denote the wt% LCP in the blend.

Fig. 2. Thermal transitions measured by DSC vs. blend composition. Open figures denote measurements made after quenching the sample rapidly from 290°C. Closed figures denote measurements made after cooling the sample at 20°C/min from 270°C: (△) Tg(LCP), (○) Tg(PC), (□) K -> N (LCP).

Fig. 3. DSC heating thermograms of LCP/PC blends after annealing at 145°C. The numbers in parentheses denote the wt% LCP in the blend.

Fig. 4. Melt viscosity vs. shear rate at 270°C for LCP/PC blends: (□) PC, (○) 95%PC/5%LCP, (■) 90%PC/10%LCP, (◇) 80%PC/20%LCP, (•) 60%PC/40%LCP, (△) 40%PC/60%LCP, (◆) 20%PC/80%LCP. (▽) LCP.

Fig. 5. Melt viscosity vs. blend composition at 270°C and a shear rate of 150 $s^{-1}$.

Fig. 6. Effect of composition on the morphology of PC/LCP blends: (a) 5% LCP, (b) 10%, (c) 20%, (d) 40%, (e) 60%, (f) 100%. All specimens were sheared with a cone and and plate rheometer at 1 $s^{-1}$.

Fig. 7. Effect of shear rate on the morphology of an 80%PC/20%LCP blend: (a) $\dot{\gamma}$ = 1 $s^{-1}$, (b) 10 $s^{-1}$, (c) 100 $s^{-1}$.

Fig. 8. Effect of deformation history on the morphology of a 80%PC/20%LCP blend: (a) sheared in a cone and plate rheometer at 10 $s^{-1}$, (b) extruded in a capillary viscometer(L/D = 40) at 75 $s^{-1}$, (c) capillary (L/D = 20) at 75 $s^{-1}$, (d) capillary (L/D = 20) at 150 $s^{-1}$, (e) capillary (L/D = 10) at 1191 $s^{-1}$, (f) melt drawn from capillary exit.

Fig. 9. Effect of drawing on the morphology of (a) 90%PC/10%LCP blend and (b) 40%PC/60%LCP blend.

Fig.10. DMTA thermograms of compression molded PC/LCP blends: (a) E', (b) tan $\delta$; (——) PC, (---) 90%PC/10%LCP, (· · · ·) 80%PC/20%LCP, (-·-·-·) 60%PC/40%LCP, (-·-·-·-·) 40%PC/60%LCP, (— — —) LCP.

Fig.11. DMTA thermograms of 90%PC/10%LCP: (----) compression molded sample, (——) drawn fiber (DR = 1000).

Fig.12. Moduli of PC/LCP blends vs. volume fraction LCP: (o) compression molded samples, (•) melt drawn samples. The solid lines correspond to the lower and upper bound predictions, equations (1) and (2), respectively.

Fig. 1.

Fig 1

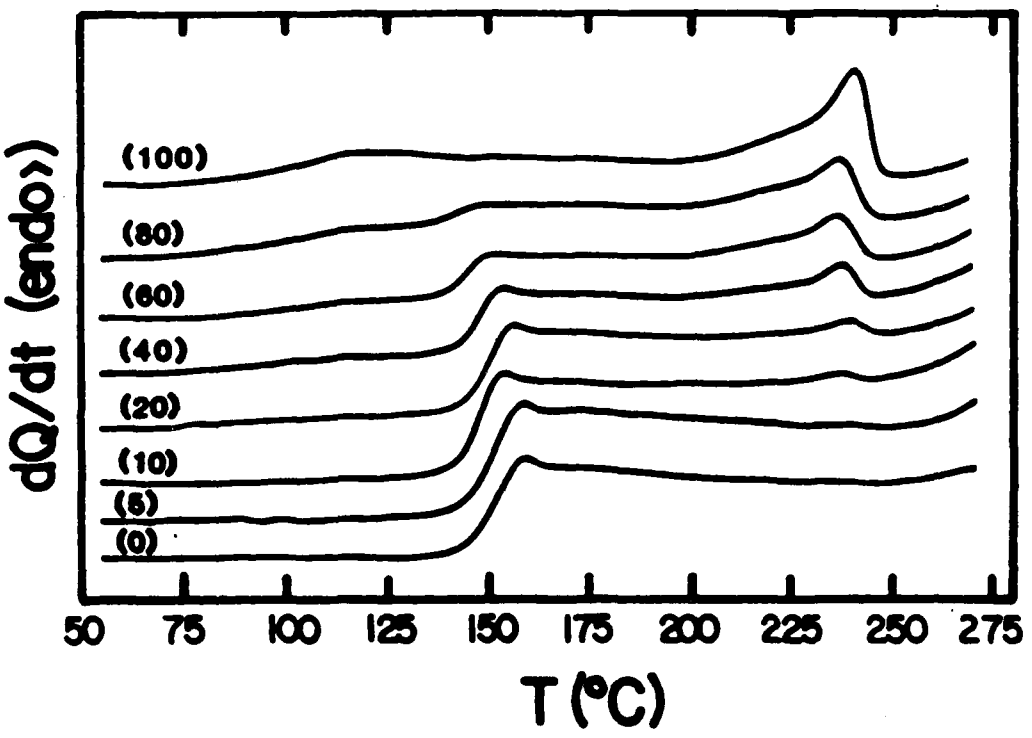
dQ/dt (endo)
(100)
(80)
(60)
(40)
(20)
(10)
(5)
(0)
50
75
100
125
150
175
200
225
250
275
T (°C)

FIG 2

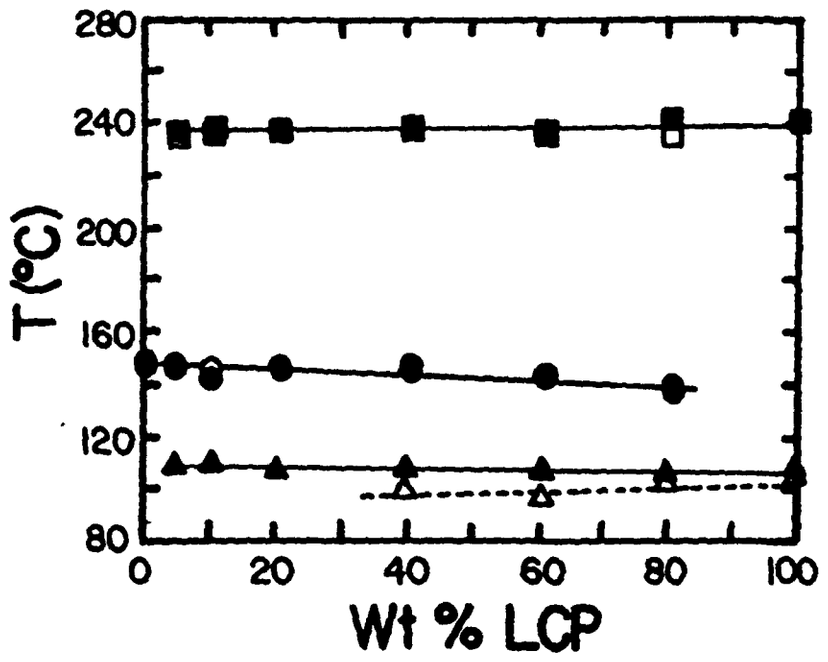

FIG 3

FIG 3

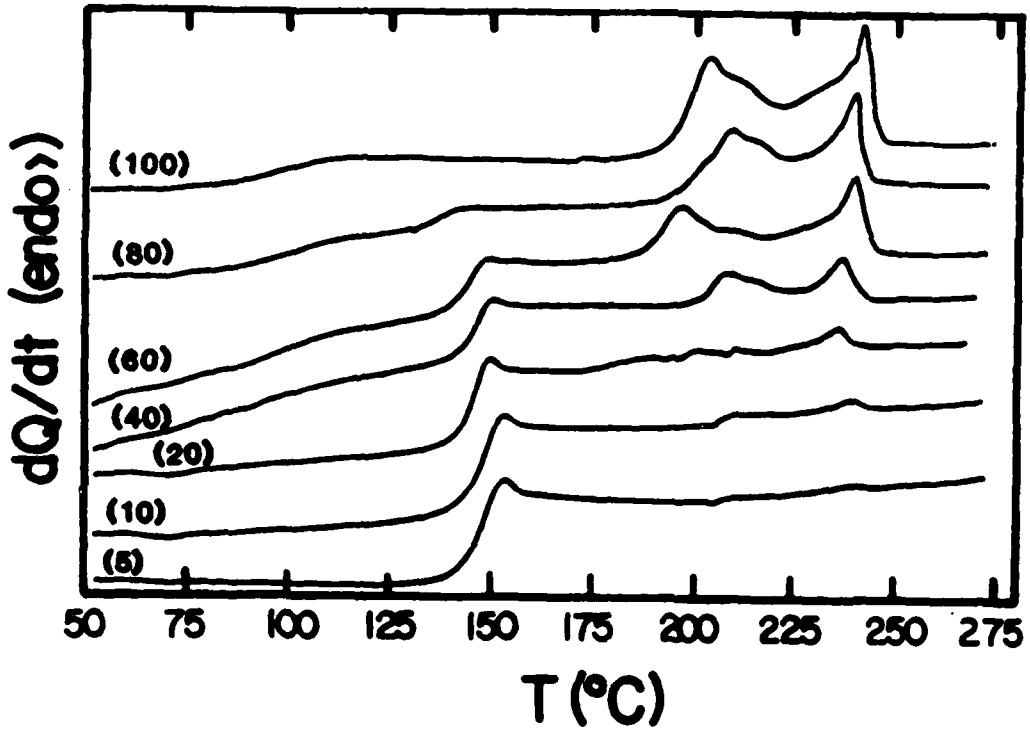
dQ/dt (endo)
(100)
(80)
(60)
(40)
(20)
(10)
(5)
50
75
100
125
150
175
200
225
250
275
T (°C)

FIG 4

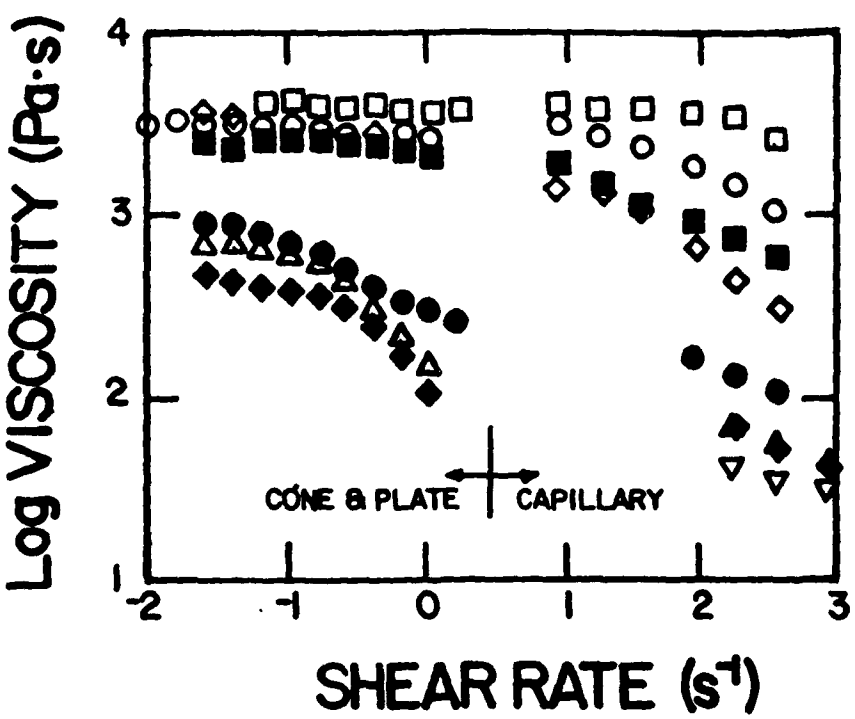
Log VISCOSITY (Pa·s)
4
3
2
1
-2
-1
0
1
2
3
CONE & PLATE
CAPILLARY
SHEAR RATE (s⁻¹)

FIG 5

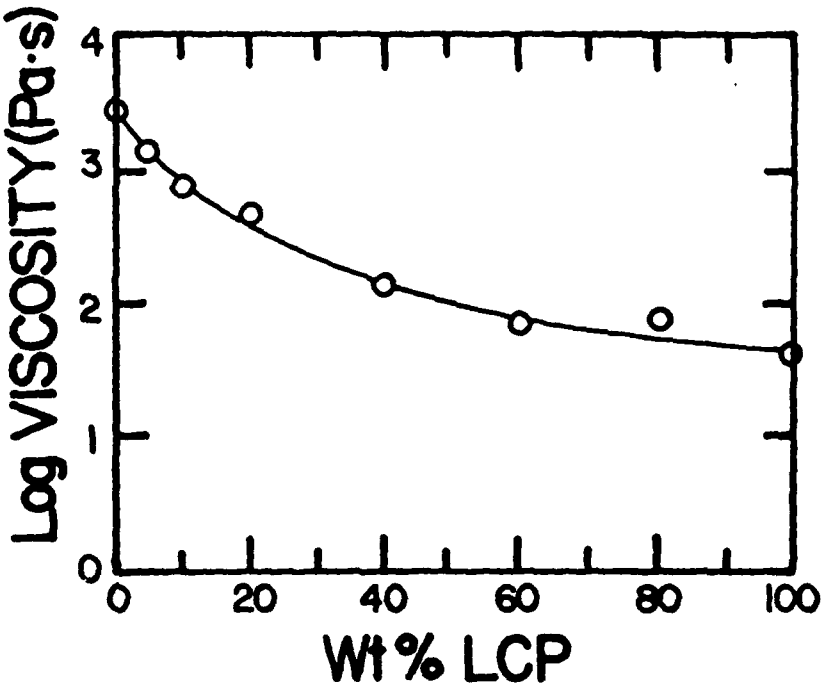


5% LCP


10% LCP


$\gamma = 1\ s^{-1}$


20% LCP


40% LCP


$\gamma = 10\ s^{-1}$


60% LCP


100% LCP

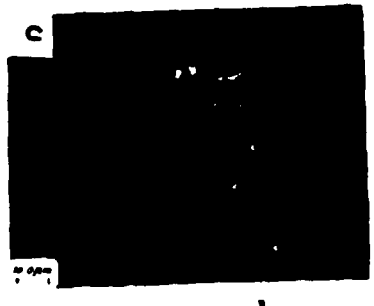


$\gamma = 100\ s^{-1}$

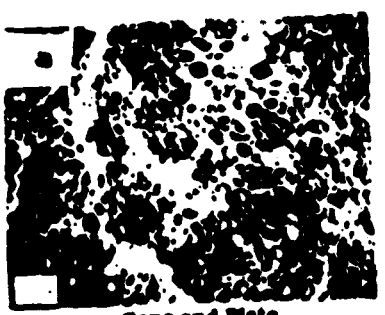


Cone and Plate
$\gamma = 10\ s^{-1}$


Capillary (L/D = 40)
$\gamma = 75\ s^{-1}$

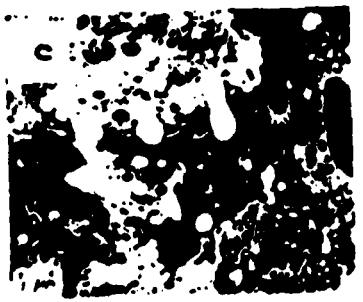


Capillary (L/D = 20)
$\gamma = 75\ s^{-1}$


Capillary (L/D = 20)
$\gamma = 150\ s^{-1}$

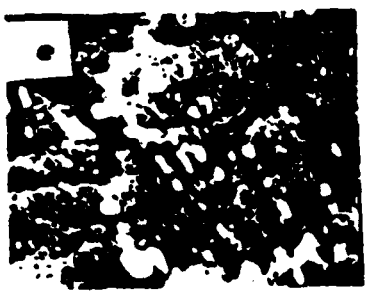


Capillary (L/D = 10)
$\gamma = 1191\ s^{-1}$


Capillary
Melt Drawn

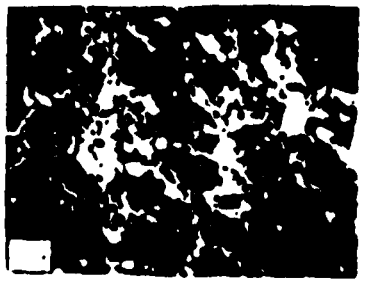

Draw Ratio ~ 50 (2K X)

a

Draw Ratio ~ 500 (2K X)

Draw Ratio ~ 50 (1K X)

b

Draw Ratio ~ 500 (1K X)

Fig 11(a)




Fig 10(a)

FIG 10(b)

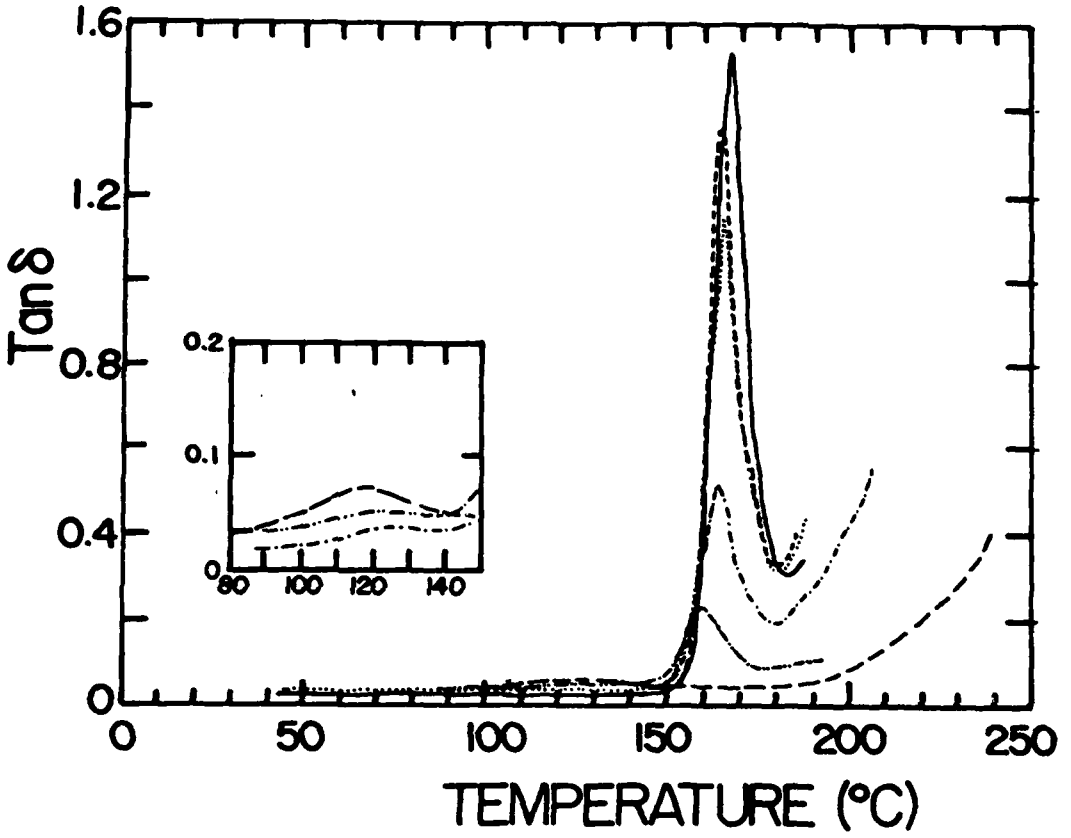
1.6
1.2
0.8
0.4
0
Tan δ
0.2
0.1
0
80
100
120
140
0
50
100
150
200
250
TEMPERATURE (°C)

Fig 11

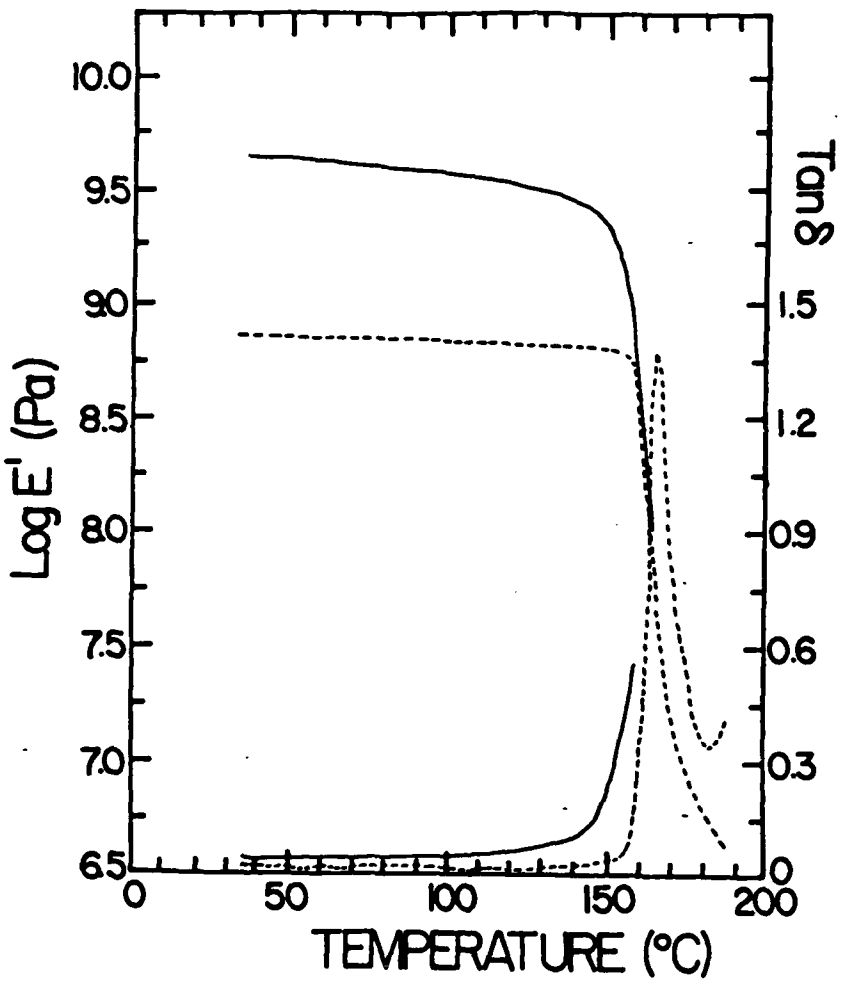
10.0
9.5
9.0
8.5
8.0
7.5
7.0
6.5
Log E' (Pa)
1.5
1.2
0.9
0.6
0.3
0
Tan δ
0
50
100
150
200
TEMPERATURE (°C)

Fig 11

Fig 12

FIG 12

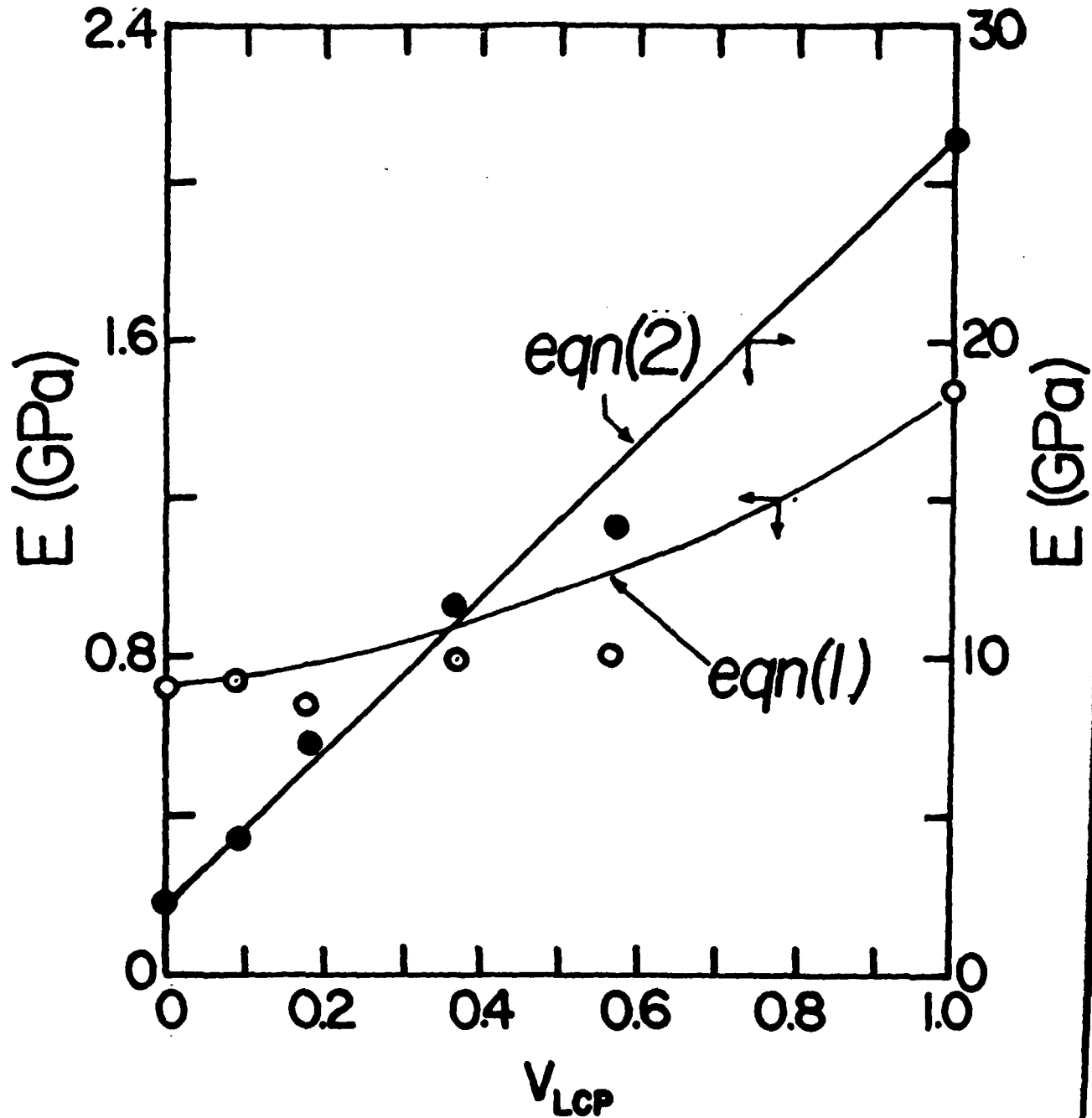

DL/1113/87/2

# TECHNICAL REPORT DISTRIBUTION LIST, GEN

| | No. Copies |
|---|---|
| Office of Naval Research<br>Attn: Code 1113<br>800 N. Quincy Street<br>Arlington, Virginia 22217-5000 | 2 |
| Dr. Bernard Douda<br>Naval Weapons Support Center<br>Code 50C<br>Crane, Indiana 47522-5050 | 1 |
| Naval Civil Engineering Laboratory<br>Attn: Dr. R. W. Drisko, Code L52<br>Port Hueneme, California 93401 | 1 |
| Defense Technical Information Center<br>Building 5, Cameron Station<br>Alexandria, Virginia 22314 | 12 high quality |
| DTNSRDC<br>Attn: Dr. H. Singerman<br>Applied Chemistry Division<br>Annapolis, Maryland 21401 | 1 |
| Dr. William Tolles<br>Superintendent<br>Chemistry Division, Code 6100<br>Naval Research Laboratory<br>Washington, D.C. 20375-5000 | 1 |
| Dr. David Young<br>Code 334<br>NORDA<br>NSTL, Mississippi 39529 | 1 |
| Naval Weapons Center<br>Attn: Dr. Ron Atkins<br>Chemistry Division<br>China Lake, California 93555 | 1 |
| Scientific Advisor<br>Commandant of the Marine Corps<br>Code RD-1<br>Washington, D.C. 20380 | 1 |
| U.S. Army Research Office<br>Attn: CRD-AA-IP<br>P.O. Box 12211<br>Research Triangle Park, NC 27709 | 1 |
| Mr. John Boyle<br>Materials Branch<br>Naval Ship Engineering Center<br>Philadelphia, Pennsylvania 19112 | 1 |
| Naval Ocean Systems Center<br>Attn: Dr. S. Yamamoto<br>Marine Sciences Division<br>San Diego, California 91232 | 1 |